

Electronic and magnetic properties of $R_{0.5}A_{0.5}\text{MnO}_3$ compounds ($R = \text{Gd, Dy, Ho, Er}$; $A = \text{Sr, Ca}$)

T. Terai, T. Sasaki, T. Kakeshita, T. Fukuda, and T. Saburi

Department of Materials Science and Engineering, Graduate School of Engineering, Osaka University, Suita, Osaka 565-0871, Japan

H. Kitagawa and K. Kindo

Research Center for Materials Science at Extreme Conditions, Osaka University, Toyonaka, Osaka 560-8531, Japan

M. Honda

Department of Physics, Faculty of Science, Naruto University of Education, Naruto, Tokushima 772-8502, Japan

(Received 5 April 1999)

Electronic and magnetic properties of the perovskitelike compounds of $R_{0.5}A_{0.5}\text{MnO}_3$ ($R = \text{Gd, Dy, Ho, Er}$; $A = \text{Sr, Ca}$) have been studied by measuring lattice parameter, electrical resistivity, magnetic susceptibility, and magnetization. All the Sr-doped compounds show a transition from a paramagnetic insulator to a spin-glass-like insulator at T_g , even though the manganite $\text{La}_{0.5}\text{Ca}_{0.5}\text{MnO}_3$, with nearly the same tolerance factor t , have been shown by others, to have different transitions. On the other hand, all the Ca-doped compounds show a charge-ordering transition at T_{CO} and show a transition from a paramagnetic insulator to a canted antiferromagnetic insulator and/or a spin-glass-like insulator at T_{CA} below T_{CO} . These transition temperatures decrease with decreasing t . In the compound of $\text{Gd}_{0.5}\text{Ca}_{0.5}\text{MnO}_3$, the collapse of the charge ordering has been observed under a pulsed high magnetic field of 45 T at 4.2 K. On the other hand, in the compound of $\text{Gd}_{0.5}\text{Sr}_{0.5}\text{MnO}_3$, the magnetization process depends on the strength of magnetic field. These electronic and magnetic properties depend not only on the tolerance factor but also the variance (second moment) of the A-site ion radii distribution.

I. INTRODUCTION

Perovskite manganites with 50% of trivalent rare-earth ions of R^{3+} replaced by divalent alkaline-earth metal ions of A^{2+} , $R_{0.5}A_{0.5}\text{MnO}_3$ ($R = \text{La, Pr, Nd, Sm}$; $A = \text{Sr, Ca}$), have been extensively studied and found to show interesting electronic and magnetic properties, such as metal-insulator transition due to the double-exchange interaction (magnetic interaction between Mn^{3+} and Mn^{4+} that is caused by the hopping of e_g electrons between the two partially filled d shells with strong on-site Hund's coupling), charge-ordering transitions due to the long-range Coulomb interaction among the carriers and antiferromagnetic transition due to the super exchange interaction, depending on the combination of R and A .¹⁻¹³

The electronic and magnetic properties of manganites investigated until now have been discussed by using a tolerance factor t , which is a geometrical index defined as $t = (r_A + r_O) / \sqrt{2}(r_{\text{Mn}} + r_O)$, where r_A is the average ionic radius of R^{3+} and A^{2+} , r_O is the ionic radius of O^{2-} , and r_{Mn} is the average ionic radius of Mn^{3+} and Mn^{4+} . With decreasing t , the Mn-O-Mn bond angles, which are microscopically related to the transfer integral b describing electron hopping between Mn^{3+} and Mn^{4+} , decrease.⁸

Recently, however, Rodriguez-Martinez and Attfield¹⁴ and Damay *et al.*¹⁵ suggest that electronic and magnetic properties of manganites depend not only on the tolerance factor, as mentioned above, but also on the variance (second moment) σ^2 defined by the equation, $\sigma^2 = \sum y_i r_i^2 - r_A^2$, where r_i is the radius of each R^{3+} and A^{2+} , y_i is their fractional

occupancies of the i ions ($\sum y_i = 1$), r_A is the average ionic radius of R^{3+} and A^{2+} , corresponding to a random distribution of Mn-O-Mn bond angles.^{14,15} In order to confirm the propriety of this suggestion, we need information on electronic and magnetic properties in other compounds of $R_{0.5}A_{0.5}\text{MnO}_3$ ($A = \text{Sr, Ca}$) with the same t but different σ^2 .^{4,5} For such experiments, the compounds including heavy rare-earth metals such as Gd, Dy, Ho, and Er are quite suitable because those $R_{0.5}A_{0.5}\text{MnO}_3$ ($A = \text{Sr, Ca}$) compounds have a t value nearly the same as that of the $\text{La}_{0.5}\text{Ca}_{0.5}\text{MnO}_3$.^{4,5} Nevertheless the former compounds have σ^2 values quite different from those of the latter compounds. However, there are not many studies on such compounds.¹⁶⁻¹⁹

The purpose of the present study, therefore, is to investigate the electronic and magnetic properties of those compounds of $R_{0.5}\text{Sr}_{0.5}\text{MnO}_3$ ($R = \text{Gd, Dy, Ho, Er}$). In addition, we investigate $R_{0.5}\text{Ca}_{0.5}\text{MnO}_3$ ($R = \text{Gd, Dy, Ho, Er}$) because we can obtain the information on the electronic and magnetic properties of manganites with a value of t lower than 0.909, whose information has also quite few properties in $R_{0.5}A_{0.5}\text{MnO}_3$.¹⁶⁻²²

II. EXPERIMENT

Polycrystalline specimens of $R_{0.5}A_{0.5}\text{MnO}_3$ ($R = \text{Gd, Dy, Ho, Er}$; $A = \text{Sr, Ca}$) were prepared by conventional solid-state reaction processing in air. Stoichiometric compounds of Gd_2O_3 , Dy_2O_3 , Ho_2O_3 , Er_2O_3 , SrCO_3 , CaCO_3 , and Mn_3O_4 were mixed for the compositions mentioned above and calcined in air by holding the specimens at 1173–1273

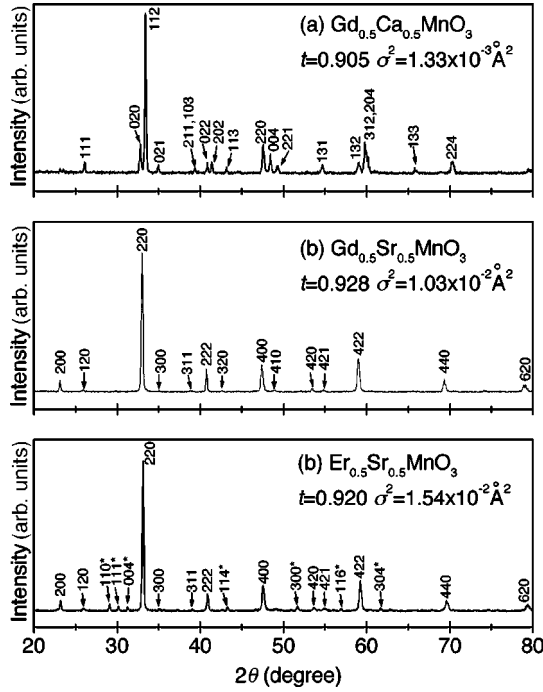


FIG. 1. X-ray-diffraction pattern at room temperature for (a) $\text{Gd}_{0.5}\text{Sr}_{0.5}\text{MnO}_3$, (b) $\text{Er}_{0.5}\text{Sr}_{0.5}\text{MnO}_3$, (c) $\text{Gd}_{0.5}\text{Ca}_{0.5}\text{MnO}_3$. The symbols (*) in (b) represent the reflections of hexagonal structure (ErMnO_3).

K for 12–15 h. Sintering was carried out in air by holding the specimens at 1653–1773 K for 25–60 h after intermediate grinding. In this paper, we describe the compounds using composition together with the tolerance factor t , and the variance σ^2 , for simplicity. In the present case, the increase in weight of rare-earth metal ions ($\text{Gd} \rightarrow \text{Dy} \rightarrow \text{Ho} \rightarrow \text{Er}$) corresponds to the decrease in t and the increase in σ^2 . Powder x-ray-diffraction measurement was made for all the compounds using Rigaku RINT 2500 and Mascience MXP³ systems. Resistivity ρ was measured by the standard four-probe method. In the measurement, current and voltage leads were connected to the specimen with silver paste. Magnetic susceptibility was measured with both a superconducting quantum interference device magnetometer and a vibrating sample magnetometer. Magnetization was measured by applying static magnetic fields of up to 1.8 T and also by applying pulsed high magnetic fields of up to 68 T, whose instrument belongs to Research Center for Materials Science at Extreme Conditions, Osaka University. Incidentally, we do not analyze the oxygen content in the specimens used in the present study, although it was reported to affect the electronic and magnetic properties in the manganites.¹⁶

III. RESULTS

A. X-ray-diffraction and electrical resistivity measurements

We made powder x-ray-diffraction measurement for all the compounds at room temperature. The reflections of all the Ca-doped compounds can be indexed by only an orthorhombic ($c/\sqrt{2} < a < b$, O'-type) structure and a typical result of $\text{Gd}_{0.5}\text{Ca}_{0.5}\text{MnO}_3$ is shown in Fig. 1(a). On the other hand, the reflections of Sr-doped compounds ($R = \text{Gd}, \text{Dy}, \text{Ho}$) seem to be different from those of the Ca-doped compounds,

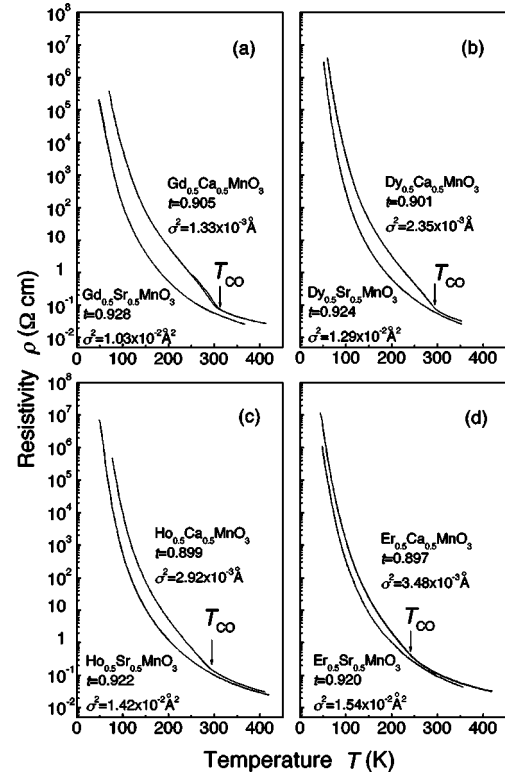


FIG. 2. Temperature dependence of resistivity for (a) $\text{Gd}_{0.5}\text{Sr}_{0.5}\text{MnO}_3$ and $\text{Gd}_{0.5}\text{Ca}_{0.5}\text{MnO}_3$, (b) $\text{Dy}_{0.5}\text{Sr}_{0.5}\text{MnO}_3$ and $\text{Dy}_{0.5}\text{Ca}_{0.5}\text{MnO}_3$, (c) $\text{Ho}_{0.5}\text{Sr}_{0.5}\text{MnO}_3$ and $\text{Ho}_{0.5}\text{Ca}_{0.5}\text{MnO}_3$, (d) $\text{Er}_{0.5}\text{Sr}_{0.5}\text{MnO}_3$ and $\text{Er}_{0.5}\text{Ca}_{0.5}\text{MnO}_3$.

as typically shown in Fig. 1(b) of $\text{Gd}_{0.5}\text{Sr}_{0.5}\text{MnO}_3$. Recently, García-Landa *et al.*¹⁷ made a precise x-ray measurement for the $\text{Gd}_{0.5}\text{Sr}_{0.5}\text{MnO}_3$ compound and found it to be an orthorhombic structure, where the difference in values of the a and b axes is quite small. This difference cannot be detected in our experiment because of the limitation of our x-ray instruments. Instead, we indexed all the reflections of the Sr-doped compounds ($R = \text{Gd}, \text{Dy}, \text{Ho}$) by regarding these compounds as a pseudocubic structure. The specimen of $\text{Er}_{0.5}\text{Sr}_{0.5}\text{MnO}_3$ consists of a pseudocubic phase with a slight amount of a hexagonal phase. The result is shown in Fig. 1(c).

Then, we measured the electrical resistivity ρ as a function of temperature for all the compounds, where the heating and cooling rate were about 0.5 K/min. The results obtained are shown in Figs. 2(a)–2(d). In each figure, the ρ - T curves of Sr- and Ca-doped compounds with the same rare-earth ions are shown for comparison. It is noted in Figs. 2(a)–2(d) that the resistivity is quite high; i.e., all the compounds are almost insulator in the measured temperature range. A characteristic feature is that the increasing ratio in electrical resistivity against temperature for all the Ca-doped compounds changes at a certain temperature (T_{CO}) indicated with an arrow in each figure, although such behavior is not observed for all the Sr-doped compounds. Similar changes in electrical resistivity have already been observed in $\text{Pr}_{1-x}\text{Ca}_x\text{MnO}_3$ ($0.3 \leq x \leq 0.5$) (Ref. 3) and $\text{La}_{0.5}\text{Ca}_{0.5}\text{MnO}_3$,⁴ and they have been confirmed to be due to an onset of charge ordering by neutron-diffraction measurement.²³ From this fact and the present result of the pulsed magnetic field measurement de-

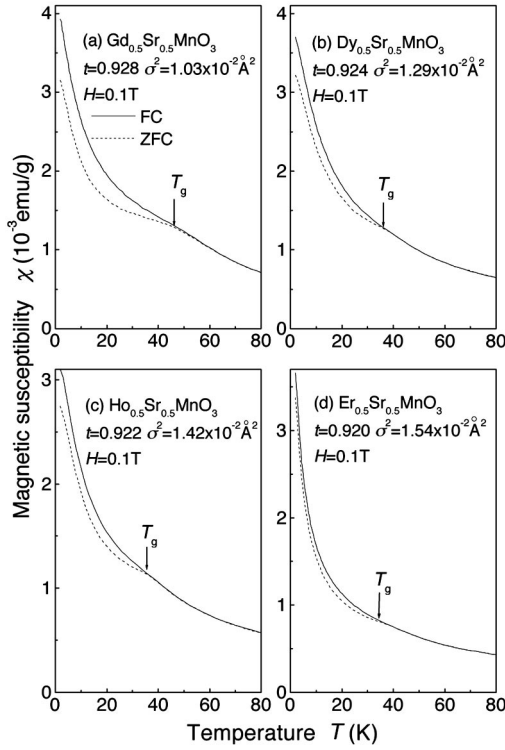


FIG. 3. Temperature dependence of magnetic susceptibility for (a) $\text{Gd}_{0.5}\text{Sr}_{0.5}\text{MnO}_3$, (b) $\text{Dy}_{0.5}\text{Sr}_{0.5}\text{MnO}_3$, (c) $\text{Ho}_{0.5}\text{Sr}_{0.5}\text{MnO}_3$, (d) $\text{Er}_{0.5}\text{Sr}_{0.5}\text{MnO}_3$, obtained by FC (solid line) and ZFC (dotted line) runs at 0.1 T.

scribed later, we find that the temperature where the increasing rate of electrical resistivity changes during cooling, corresponds to the onset temperature of the charge-ordering transition. Another feature is that the charge-ordering temperature decreases with decreasing t , i.e., in order of the compounds, including heavier rare-earth elements (Gd, Dy, Ho, Er). This transition has a temperature hysteresis as seen in the figure, indicating that the transition is of a first order.

B. Magnetic susceptibility measurement

In order to obtain the information on magnetic states for all the compounds, the magnetic susceptibility (χ) measurements have been done under the two conditions; one is a zero-field-cooled (ZFC) run and the other is a field-cooled (FC) run at $H = 3 \times 10^{-4} \sim 5 \times 10^{-1}$ T. The results are shown in Figs. 3(a)–3(d) and Figs. 4(a)–4(d) for the Sr-doped and Ca-doped compounds, respectively. In the figures, solid and dotted curves represent the results of FC and ZFC runs, respectively.

In Figs. 3(a)–3(d), the susceptibility decreases with increasing temperature for all the Sr-doped compounds. The relations between $1/\chi$ and T are almost linear at temperatures higher than 100 K for all the Sr-doped compounds. The effective moments obtained from the relations are in good agreement with calculated ones for all the compounds, where the magnetic moment of a rare-earth metal ion is considered. The results are shown in Table I. It is noted in Fig. 3 that the temperature dependence of χ obtained by the ZFC run is different from that obtained by the FC run at temperatures lower than T_g for all the compounds, suggesting that these

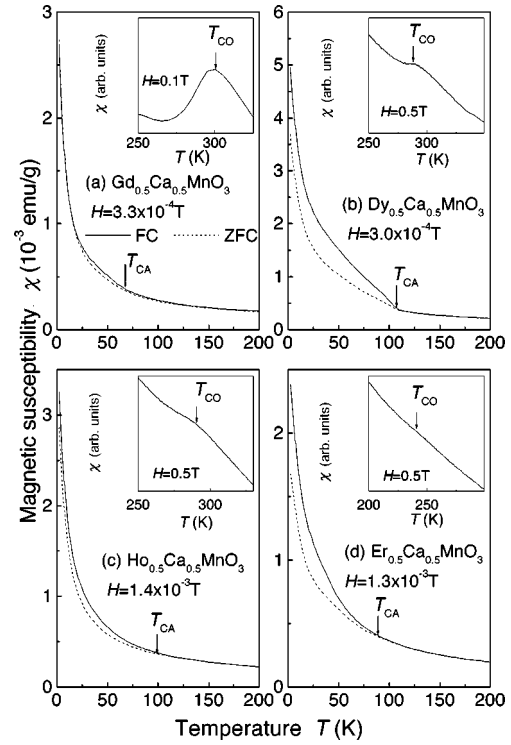


FIG. 4. Temperature dependence of magnetic susceptibility for (a) $\text{Gd}_{0.5}\text{Ca}_{0.5}\text{MnO}_3$, (b) $\text{Dy}_{0.5}\text{Ca}_{0.5}\text{MnO}_3$, (c) $\text{Ho}_{0.5}\text{Ca}_{0.5}\text{MnO}_3$, (d) $\text{Er}_{0.5}\text{Ca}_{0.5}\text{MnO}_3$, obtained by FC (solid line) and ZFC (dotted line) runs at $3.0 \times 10^{-4} \sim 1.4 \times 10^{-3}$ T. Insets show the temperature dependence of magnetic susceptibility at 0.1–0.5 T.

compounds are in a spin-glass-like state at temperatures lower than T_g . This spin-glass-like state was already reported in $\text{Gd}_{0.5}\text{Sr}_{0.5}\text{MnO}_3$ by García-Landa *et al.*¹⁷ by using neutron-diffraction and ac susceptibility measurements.

In Figs. 4(a)–4(d), the susceptibility also decreases with increasing temperature for all the Ca-doped compounds. The relations between $1/\chi$ and T are almost linear at temperatures between 150 K and T_{CO} for all the Ca-doped compounds. The effective moments obtained from the relations are in good agreement with calculated ones for all the compounds, where the magnetic moments of rare-earth metal ions are considered, as in the Sr-doped compounds. The results are also shown in Table I. A characteristic feature in Fig. 4 is that the temperature dependence of χ obtained by ZFC runs is quite different from that obtained by a FC run at temperatures lower than the temperature indicated with T_{CA} for all

TABLE I. Experimental and calculated effective magnetic moments in $R_{0.5}A_{0.5}\text{MnO}_3$ ($R = \text{Gd, Dy, Ho, Er}$; $A = \text{Sr, Ca}$).

Compounds	Experiment (μ_B)	Calculation (μ_B)
$\text{Gd}_{0.5}\text{Sr}_{0.5}\text{MnO}_3$	8.57	8.36
$\text{Dy}_{0.5}\text{Sr}_{0.5}\text{MnO}_3$	9.90	9.72
$\text{Ho}_{0.5}\text{Sr}_{0.5}\text{MnO}_3$	9.95	9.69
$\text{Er}_{0.5}\text{Sr}_{0.5}\text{MnO}_3$	9.18	9.18
$\text{Gd}_{0.5}\text{Ca}_{0.5}\text{MnO}_3$	8.52	8.36
$\text{Dy}_{0.5}\text{Ca}_{0.5}\text{MnO}_3$	9.62	9.72
$\text{Ho}_{0.5}\text{Ca}_{0.5}\text{MnO}_3$	9.30	9.69
$\text{Er}_{0.5}\text{Ca}_{0.5}\text{MnO}_3$	9.19	9.18

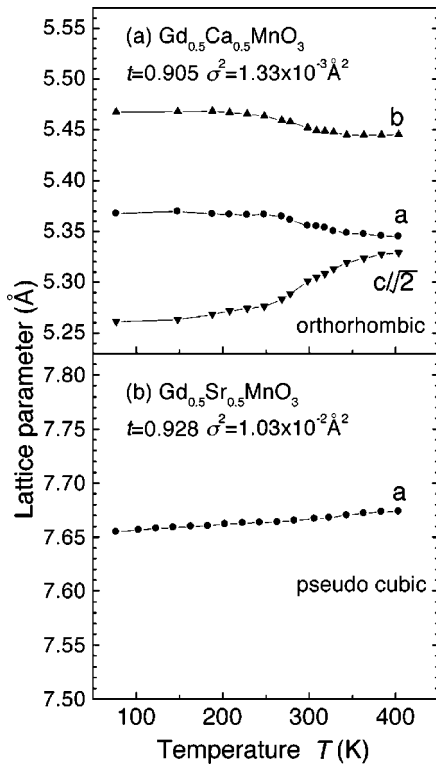


FIG. 5. Temperature dependence of lattice parameters for (a) $\text{Gd}_{0.5}\text{Ca}_{0.5}\text{MnO}_3$, (b) $\text{Gd}_{0.5}\text{Sr}_{0.5}\text{MnO}_3$.

the compounds. This suggests that the magnetic states of Ca-doped compounds are also in a spin-glass-like state at these lower temperatures, as in a way similar to the Sr-doped compounds. However, recent studies by Tomioka *et al.*⁷ and Blasco *et al.*¹⁹ show that $R_{0.5}\text{Ca}_{0.5}\text{MnO}_3$ ($R=\text{Sm}, \text{Tb}$) compounds with nearly the same t as that of the present $R_{0.5}\text{Ca}_{0.5}\text{MnO}_3$ ($R=\text{Gd}, \text{Dy}, \text{Ho}, \text{Er}$) compounds exhibit an antiferromagnetic transition. Considering these results, the magnetic state of the present Ca-doped compounds is believed to be a canted antiferromagnetic rather than a spin-glass state.

It should be noted that the change in χ due to the charge ordering is not clear although the change in ρ due to this ordering is clear, as seen in Figs. 2(a)–2(d). Since the change due to charge ordering is considered to be proportional to the strength of magnetic field, we applied higher magnetic fields to the Ca-doped compounds to check it. The results are shown in the inset on each figure. As known from the inset in each figure, the increasing ratio of χ clearly changes at the temperature indicated with an arrow on each curve. This temperature coincides with the charge-ordering temperature determined by electrical resistivity measurements for all the compounds.

C. Collapse of charge ordering under a high magnetic field

As mentioned above, the Ca-doped compounds used in the present study exhibit the charge ordering transition. It has been known the charge-ordered state collapses by application of high magnetic field (for example, 25 T at 4.2 K for $\text{Nd}_{0.5}\text{Ca}_{0.5}\text{MnO}_3$).²⁴ In order to confirm the collapse of the charge ordering in the present Ca-doped compounds, we applied a pulsed high magnetic field to it. In the experiment, we

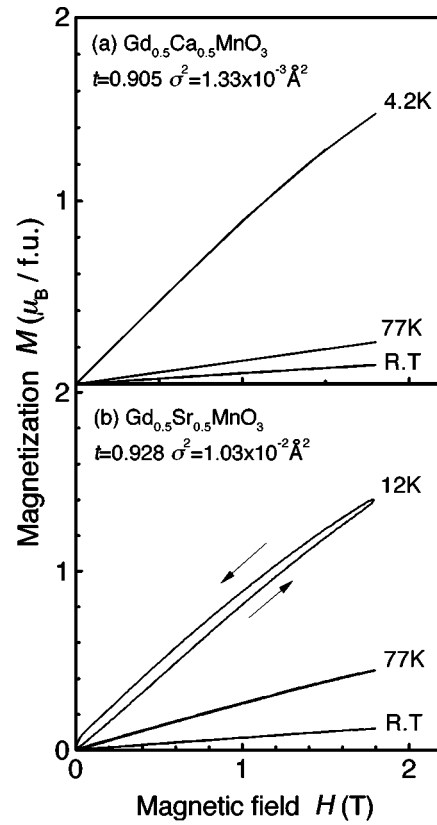


FIG. 6. Magnetization curves for (a) $\text{Gd}_{0.5}\text{Ca}_{0.5}\text{MnO}_3$, (b) $\text{Gd}_{0.5}\text{Sr}_{0.5}\text{MnO}_3$, obtained under magnetic fields of up to 1.8 T at 4.2, 12, 77 K and RT.

chose $\text{Gd}_{0.5}\text{Ca}_{0.5}\text{MnO}_3$ ($t=0.905$) because the change in ρ and χ against temperature is largest among the Ca-doped compounds used in the present study. Before doing such experiment, we examined the initial states of $\text{Gd}_{0.5}\text{Ca}_{0.5}\text{MnO}_3$, such as crystal structure and magnetization process, at low temperatures. Figure 5(a) shows the lattice parameter as a function of temperature for $\text{Gd}_{0.5}\text{Ca}_{0.5}\text{MnO}_3$. As known from the figure, the $\text{Gd}_{0.5}\text{Ca}_{0.5}\text{MnO}_3$ has the large change in the lattice parameters around 320 K, which nearly corresponds to T_{CO} determined by electrical resistivity and magnetic susceptibility measurements, as mentioned before. Figure 6(a) shows the magnetization curves of $\text{Gd}_{0.5}\text{Ca}_{0.5}\text{MnO}_3$ under low magnetic fields of up to 1.8 T at RT, 77 K and 4.2 K, where there is no hysteresis, at each temperature. Then we applied a pulsed high magnetic field to $\text{Gd}_{0.5}\text{Ca}_{0.5}\text{MnO}_3$ at the temperatures of 200 and 4.2 K below T_{CO} and the results are shown in Fig. 7. As known from the figure, a sudden increase in magnetization is observed at 45 T (4.2 K) and 30 T (200 K), indicated with arrows, and there exists hysteresis at both temperatures. Similar behavior has been observed in $\text{Pr}_{0.5}\text{Ca}_{0.5}\text{MnO}_3$ and $\text{Nd}_{0.5}\text{Ca}_{0.5}\text{MnO}_3$ compounds by Tokunaga *et al.*²⁴ and this has been explained by the collapse of the charge ordering. Considering the present and Tokunaga *et al.*'s results, we believe that this sudden increase is caused by the collapse of the charge ordering. The saturated moment at 4.2 K is about $6.5\mu_{\text{B}}/\text{f.u.}$, which is in good agreement with a calculated one including the moment of Gd^{3+} .

We also applied a high magnetic field to the Sr-doped compound including the same Gd^{3+} ($\text{Gd}_{0.5}\text{Sr}_{0.5}\text{MnO}_3$, t

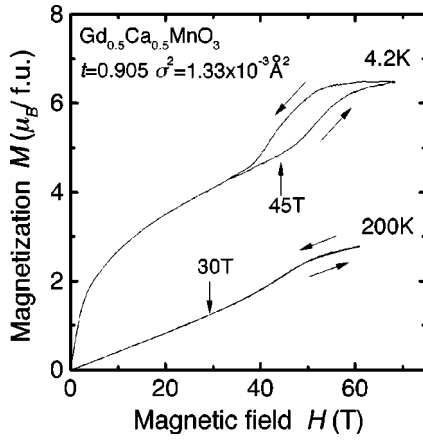


FIG. 7. Magnetization curves of $\text{Gd}_{0.5}\text{Ca}_{0.5}\text{MnO}_3$, obtained under magnetic fields of up to 68 T at 4.2 and 200 K.

$=0.928$), which has T_g at 62 K. Before doing the experiment, we measured the lattice parameter and magnetization under low magnetic field and their results are shown in Fig. 5(b) and Fig. 6(b), respectively. It is noted in Fig. 5(b) the lattice parameter decreases linearly with decreasing temperature (we regard the structure as the pseudocubic one in the present study). A characteristic feature in Fig. 6(b) is that there exists the magnetization hysteresis at 12 K ($< T_g$), but not at 77 K and RT ($> T_g$), being consistent with the result shown in Fig. 3. Then we applied pulsed high magnetic fields with a strength of 7.5 and/or 60 T at 4.2 K to the $\text{Gd}_{0.5}\text{Sr}_{0.5}\text{MnO}_3$. Their results are shown in Fig. 8 with the dotted (7.5 T) and solid (60 T) curves. As seen from the figure, the magnetization process is quite different when compared with each other, meaning that the magnetization process of $\text{Gd}_{0.5}\text{Sr}_{0.5}\text{MnO}_3$ depends on the strength of magnetic field. Such behavior is not observed at temperature 200 K, which is higher than T_g , as shown in Fig. 8. These results suggest the magnetic state of $\text{Gd}_{0.5}\text{Sr}_{0.5}\text{MnO}_3$ at 4.2 K has several metastable states. This is consistent with the fact that the magnetic state of $\text{Gd}_{0.5}\text{Sr}_{0.5}\text{MnO}_3$ is spin-glass state, as mentioned before.

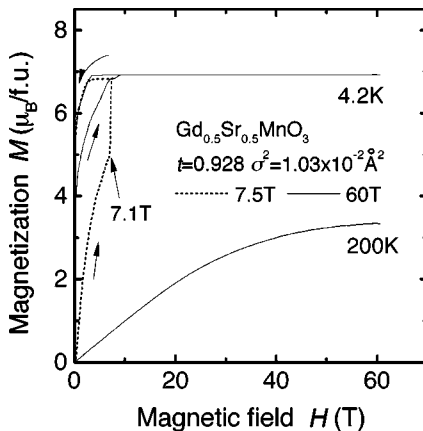


FIG. 8. Magnetization curves of $\text{Gd}_{0.5}\text{Sr}_{0.5}\text{MnO}_3$, obtained under magnetic fields of up to 60 and/or 7.5 T at 4.2 K and 60 T at 200 K. Solid and dotted lines represent magnetization curves under magnetic fields of 60 and 8 T, respectively.

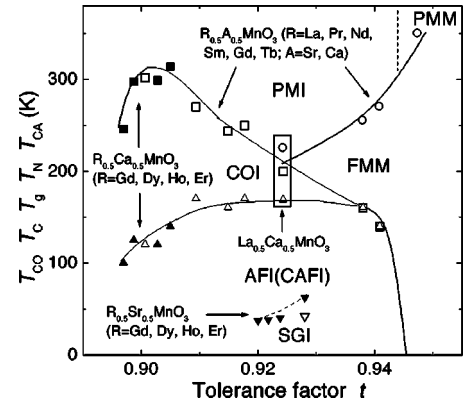


FIG. 9. Electronic and magnetic phase diagram: T_{CO} (open and closed square), T_C (open circle), T_g (inverted open and closed triangle), T_N (open triangle), and T_{CA} (closed triangle) as a function of t . Closed symbols denote for the present $R_{0.5}A_{0.5}\text{MnO}_3$ ($R=\text{Gd, Dy, Ho, Er}$; $A=\text{Sr, Ca}$) and open symbols denote for the previous $R_{0.5}A_{0.5}\text{MnO}_3$ ($R=\text{La, Pr, Nd, Sm, Gd, Tb}$; $A=\text{Sr, Ca}$). PMI, COI, FMM, SGI, AFI, and CAFI represent paramagnetic insulator, charge-ordering insulator, ferromagnetic metal, spin-glass insulator, antiferromagnetic insulator, and canted antiferromagnetic insulator, respectively.

IV. DISCUSSION

We summarized the plots of electronic and magnetic properties of the present compounds against the tolerance factor t , calculated by referring to the ion radii obtained by Shannon.²⁵ The results are shown in Fig. 9, where those obtained by other workers on $R_{0.5}A_{0.5}\text{MnO}_3$ ($R=\text{La, Pr, Nd, Sm, Gd, Tb, Y}$; $A=\text{Sr, Ca}$) by now^{2-7,17-19,24} are also shown. In the figure, T_{CO} (open and closed square), T_C (open circle), T_g (inverted open and closed triangle), T_N (open triangle), and T_{CA} (closed triangle) represent charge-ordering, Curie, spin-glass, Néel, and canted antiferromagnetic temperatures, respectively (closed symbols are of the present data). We also calculated the σ^2 (a parameter corresponding to a random distribution of Mn-O-Mn bond angles) of the present and the other manganites and added in Fig. 10 (closed symbols are of the present data).

From Figs. 9 and 10, we notice that the present $R_{0.5}\text{Sr}_{0.5}\text{MnO}_3$ ($R=\text{Gd, Dy, Ho, Er}$), which are nearly the same in t values but different in σ^2 values compared to

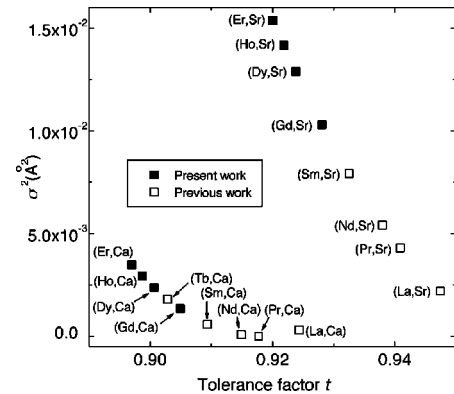


FIG. 10. Variation of σ^2 vs t for the present and previous $R_{0.5}A_{0.5}\text{MnO}_3$ compounds. The corresponding A-site cations are labeled on the graph.

$\text{La}_{0.5}\text{Ca}_{0.5}\text{MnO}_3$, show the electrical and magnetic transitions different from those of the $\text{La}_{0.5}\text{Ca}_{0.5}\text{MnO}_3$ compound. That is, $R_{0.5}\text{Sr}_{0.5}\text{MnO}_3$ ($R = \text{Gd, Dy, Ho, Er}$) compounds show a transition from a paramagnetic insulator to a spin-glass insulator while the $\text{La}_{0.5}\text{Ca}_{0.5}\text{MnO}_3$ compound shows a transition from a paramagnetic to a ferromagnetic insulator, and then to a charge-ordering and, finally, to an antiferromagnetic insulator. This result clearly suggests that electronic and magnetic properties depend not only on t but also on σ^2 , which is suggested by Rodriguez-Martinez and Attfield¹⁴ and Damay *et al.*¹⁵ Moreover, considering a large value of σ^2 , it may be quite reasonable that $R_{0.5}\text{Sr}_{0.5}\text{MnO}_3$ ($R = \text{Gd, Dy, Ho, Er}$) exhibits spin-glass states. The reason is that a large value of σ^2 corresponds to a random distribution of the Mn-O-Mn bond angles closely related to the transfer integer b . Considering this randomness of b , we can speculate that the specimen is inhomogeneous magnetically, which consists of ferromagnetic region and antiferromagnetic region depending on the value of the transfer integral, b as suggested by Teresa *et al.*¹⁰ This situation is regarded as the spin-glass state, as obtained in the present study.

It is also noted in Fig. 9 that the behavior of T_{CO} against t of the present Ca-doped compounds is quite different from that of the previous Ca-doped compounds. The relation between T_{CO} and t of the light rare-earth $R_{0.5}\text{A}_{0.5}\text{MnO}_3$ ($R = \text{La, Pr, Nd, Sm}$; $\text{A} = \text{Sr, Ca}$) compounds was explained qualitatively by the tolerance factor t as follows. That is, with decreasing t , Mn-O-Mn bond angles decrease; i.e.,

transfer integral b decreases. Therefore, e_g electrons tend to transfer from the itinerant state to the localized state with decreasing t , leading to an increase in T_{CO} , as seen in the figure. From the viewpoint of tolerance factor, the behavior of T_{CO} against t of the present Ca-doped compounds contradicts with the above explanation; i.e., T_{CO} of the present Ca-doped compounds decreases with decreasing t . This contradiction is also explained by taking the σ^2 in consideration. That is, as known in Fig. 10, the σ^2 values of the present Ca-doped compounds increase with decreasing t . Because of the high value of σ^2 , the specimen is inhomogeneous electronically, as mentioned above. Therefore, a long-range charge-ordered state comes to be difficult to realize, causing a decrease in charge-ordering temperature with decreasing t . We also believe that the decrease in T_{CA} with decreasing t in the present Ca-doped compounds is related to the increase in σ^2 with decreasing t .

From the above results, we conclude that the variance (second moment) of the A-site ion radii distribution, σ^2 , also plays an important role to determine the electronic and magnetic properties of manganites as well as tolerance factor t .

ACKNOWLEDGMENTS

The present study was supported (in part) by a Grant-in-Aid for Scientific Research of Priority Areas given by the Ministry of Education, Science, Sports and Culture, Japan. The support is greatly appreciated.

- ¹G.H. Jonker and J.H. van Santen, *Physica* (Amsterdam) **16**, 337 (1950).
- ²Y. Tomioka, A. Asamitsu, Y. Moritomo, H. Kuwahara, and Y. Tokura, *Phys. Rev. Lett.* **74**, 5108 (1995).
- ³Y. Tomioka, A. Asamitsu, H. Kuwahara, Y. Moritomo, and Y. Tokura, *Phys. Rev. B* **53**, 1689 (1996).
- ⁴P.G. Radaelli, D.E. Cox, M. Marezio, S-W. Cheong, P.E. Schiffer, and A.P. Ramirez, *Phys. Rev. Lett.* **75**, 4488 (1995).
- ⁵C.H. Chen and S-W. Cheong, *Phys. Rev. Lett.* **76**, 4042 (1996).
- ⁶H. Kuwahara, Y. Tomioka, A. Asamitsu, Y. Moritomo, and Y. Tokura, *Science* **270**, 961 (1995).
- ⁷Y. Tomioka, H. Yoshizawa, and N. Miura, *Solid State Phys.* **32**, 326 (1997).
- ⁸H.Y. Hwang, S-W. Cheong, P.G. Radaelli, M. Marezio, and B. Batlogg, *Phys. Rev. Lett.* **75**, 914 (1995).
- ⁹A. Urushibara, Y. Moritomo, T. Arima, A. Asamitsu, G. Kido, and Y. Tokura, *Phys. Rev. B* **51**, 14 103 (1995).
- ¹⁰J.M. De Teresa, M.R. Ibarra, J. Garcia J. Blasco, C. Ritter, P.A. Algarabel, C. Marquina, and A. del Moral, *Phys. Rev. Lett.* **76**, 3392 (1996).
- ¹¹C. Zener, *Phys. Rev.* **82**, 403 (1951).
- ¹²P-G. de Gennes, *Phys. Rev.* **118**, 141 (1960).
- ¹³P.W. Anderson and H. Hasegawa, *Phys. Rev.* **100**, 675 (1955).
- ¹⁴L.M. Rodriguez-Martinez and J.P. Attfield, *Phys. Rev. B* **54**, 15 622 (1996).
- ¹⁵F. Damay, C. Martin, A. Maignan, and B. Raveau, *J. Appl. Phys.* **82**, 6181 (1997).
- ¹⁶A. Barnabé, M. Hervieu, C. Martin, A. Maignan, and B. Raveau, *J. Appl. Phys.* **84**, 5506 (1998).
- ¹⁷B. García-Landa, J.M. De Teresa, M.R. Ibarra, C. Ritter, R. Drost, and M.R. Lees, *J. Appl. Phys.* **83**, 7664 (1998).
- ¹⁸A. Arulraj, P.N. Santhosh, R.S. Gopalan, A. Guha, A.K. Raychaudhuri, N. Kumar, and C.N.R. Rao, *J. Phys.: Condens. Matter* **10**, 8497 (1998).
- ¹⁹J. Blasco, J. García, J.M. De Teresa, M.R. Ibarra, J. Pérez, P.A. Algarabel, C. Marquina, and C. Ritter, *J. Phys.: Condens. Matter* **9**, 10 321 (1997).
- ²⁰P.M. Woodward, T. Vogt, D.E. Cox, A. Arulraj, C.N.R. Rao, P. Karen, and A.K. Cheetham, *Chem. Mater.* **10**, 3652 (1998).
- ²¹E. Pollert, S. Krupička, and E. Kuzmičová, *J. Phys. Chem. Solids* **43**, 1137 (1982).
- ²²N. Kumar and C.N.R. Rao, *J. Solid State Chem.* **129**, 363 (1997).
- ²³H. Yoshizawa, H. Kawano, Y. Tomioka, and Y. Tokura, *Phys. Rev. B* **52**, 13 145 (1995).
- ²⁴M. Tokunaga, N. Miura, Y. Tomioka, and Y. Tokura, *Phys. Rev. B* **57**, 5259 (1998).
- ²⁵R.D. Shannon, *Acta Crystallogr., Sect. A: Cryst. Phys., Diff., Theor. Gen. Crystallogr.* **32**, 751 (1976).